ELSEVIER

Journal of Materials Processing Technology 180 (2006) 221–232

Journal of Materials Processing Technology

www.elsevier.com/locate/jmatprotec

An assessment of finite element software for application to the roll-forming process

M.A. Sheikh *, R.R. Palavilayil

School of Mechanical, Aerospace & Civil Engineering, The University of Manchester, Sackville Street Building, Sackville Street, Manchester M60 1QD, UK

Received 23 August 2005; received in revised form 8 June 2006; accepted 9 June 2006

Abstract

The roll forming industry has many difficulties in product development and process set-up. The design and development of rolls and processes are mainly based on trial-and-error and past experiences. Recent industrial trends demand products having high quality and tight tolerances. This requires more precise and cost-effective roll-forming processes than the ones employed in the traditional product development methods.

SHAPE is a reliable FE based solution provider, which covers a wide range of roll forming and rotary forming simulations including ring rolling, tube spinning, flow forming, and thread rolling. It also provides powerful analysis tools for heat transfer, roll stress and microstructure analyses. In this chapter the technical capability of SHAPE for roll forming is assessed by studying an industrial problem. The accuracy and robustness of the software is evaluated using machine shop results.

Keywords: Manufacturing processes; Roll forming; Finite element modelling

1. Introduction

1.1. Roll-forming process

Roll forming is the process of gradually forming a flat strip of sheet metal through pairs of rolls without changing the thickness [1]. It is a progressive motion process of forming flat strip of cold metal through several stages of bending as shown in Fig. 1. The metal strip is bent by passing through a series of rolls. The process adds both stiffness and strength to the roll formed material. The products of roll-forming process are channels, gutters, siding, panels, frames, pipes and tubing, etc. The tolerances, spring-back, tearing and buckling of the strip are some of the critical parameters which have to be considered during roll forming simulations [2].

1.2. Mathematical analysis of roll forming

The curved surface of contact for the rolls makes the computation of forces and stress distribution involved in the roll-forming process very complicated. This slab method of analysis [3] considers the system analogous to a fluid flowing through a converging channel as shown in Fig. 2. Here, the volume rate of metal flows is kept constant by increasing the velocity of the strip as it moves through the roll gap.

Let,

h_o: thickness of the strip entering the roll gap;
h_f: the reduced thickness of the strip;
V_r: the surface speed of the roll;
V_o: the velocity of the strip at the entrance;
V_f: the velocity of the strip at the exit.

As V_r is constant while the velocity of the strip changes, sliding occurs between the roll and the strip. The point of the arc of contact at which the velocity of the strip is equal to the velocity of the roll is referred to as the neutral point or the no-slip point. The neutral point sets the boundary between the region of the workpiece where the roll moves faster than the workpiece and the region where the workpiece moves faster than the roll.

The frictional forces acting on the strip surface are greater in the region where the roll moves faster than the workpiece. The difference between the frictional forces in the two regions produces a net frictional force that pulls the strip into the roll

* Corresponding author.
E-mail address: m.sheikh@manchester.ac.uk (M.A. Sheikh).

0924-0136/$ – see front matter © 2006 Elsevier B.V. All rights reserved.
doi:10.1016/j.jmatprotec.2006.06.009

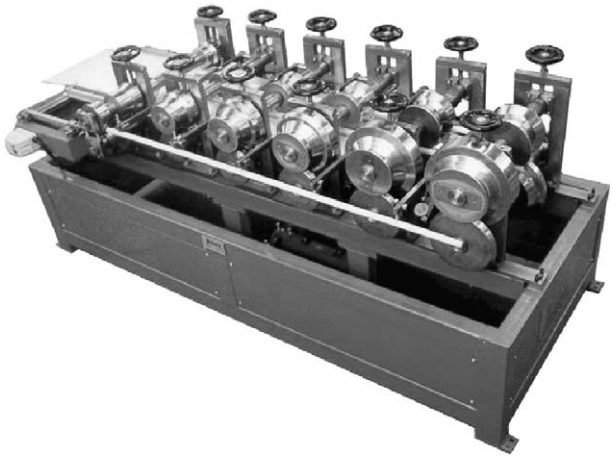

Fig. 1. A roll forming line.

gap. The net frictional force must be in the same direction as the roll velocity so that work is supplied to the workpiece. Hence, the neutral point should be located towards the exit.

A measure of the relative velocities involved is defined as the forward slip:

$$\text{Forward slip} = \frac{V_\text{f} - V_\text{r}}{V_\text{r}} \tag{1}$$

The stresses acting on an element in the entry and exit zones, respectively, are shown in Fig. 3.

Balancing the horizontal forces in the entry zone:

$$(\sigma_x + \partial\sigma_x)(h + \mathrm{d}h) - 2pR\partial\phi \sin\phi - \sigma_x h + 2\mu pR\partial\phi \cos\phi = 0 \tag{2}$$

where 'R' is the radius of the roll.

Balancing the horizontal forces in the exit zone:

$$(\sigma_x+\partial\sigma_x)(h+\mathrm{d}h) - 2pR\partial\phi \sin\phi - \sigma_x h - 2\mu pR\partial\phi \cos\phi = 0 \tag{3}$$

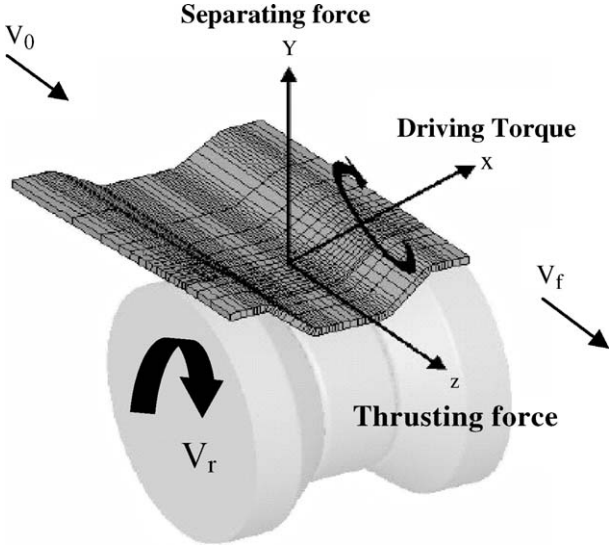

Fig. 2. Roll forming force system.

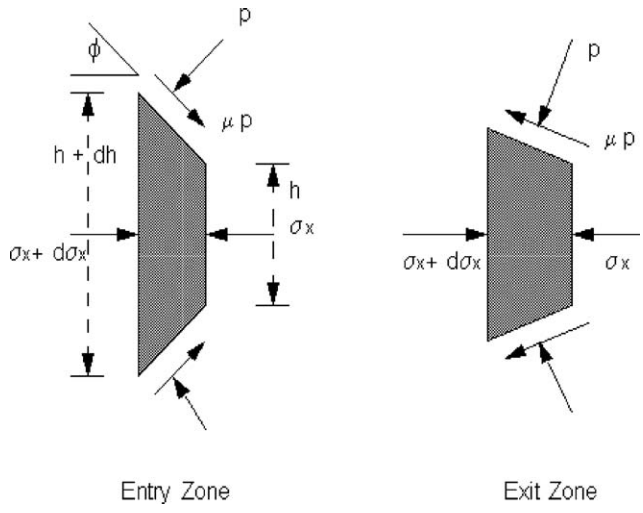

Fig. 3. Stresses on the element during roll forming.

Neglecting the second-order terms and rearranging, the above equations are modified as:

$$\frac{\mathrm{d}(\sigma_x h)}{\mathrm{d}\phi} = 2pR(\phi - \mu) \tag{4}$$

$$\frac{\mathrm{d}(\sigma_x h)}{\mathrm{d}\phi} = 2pR(\phi + \mu) \tag{5}$$

Since the angles involved are small, p is assumed to be a principal stress. Hence, the relationship between the two principal stresses and the flow stress Y_f of the material can be established as:

$$p - \sigma_x = \left[\frac{2}{3^{0.5}}\right] Y_f = Y'_f \tag{6}$$

The flow stress Y_f in Eq. (6) corresponds to the strain that the material has undergone at that particular location in the roll gap. Substituting for σ_x as a function of p and Y'_f in Eqs. (4) and (5), and after some manipulations, the following differential equations for p/Y'_f are obtained:

$$\frac{\mathrm{d}(p/Y'_\text{f})}{\mathrm{d}\phi} = \left(\frac{p}{Y'_\text{f}}\right)\left(\frac{2R}{h}\right)(\phi - \mu) \tag{7}$$

$$\frac{\mathrm{d}(p/Y'_\text{f})}{\mathrm{d}\phi} = \left(\frac{p}{Y'_\text{f}}\right)\left(\frac{2R}{h}\right)(\phi + \mu) \tag{8}$$

If h_f is the final thickness of the workpiece, h can be written as:

$$h = h_\text{f} + 2R(1 - \cos\phi)$$

or

$$h = h_\text{f} + R\phi^2 \tag{9}$$

Substituting for h in Eqs. (7) and (8), and solving for p:

$$p = KY'_\text{f}\left(\frac{h}{R}\right)\mathrm{e}^{-\mu H} \quad \text{and} \quad p = KY'_\text{f}\left(\frac{h}{R}\right)\mathrm{e}^{\mu H} \tag{10}$$

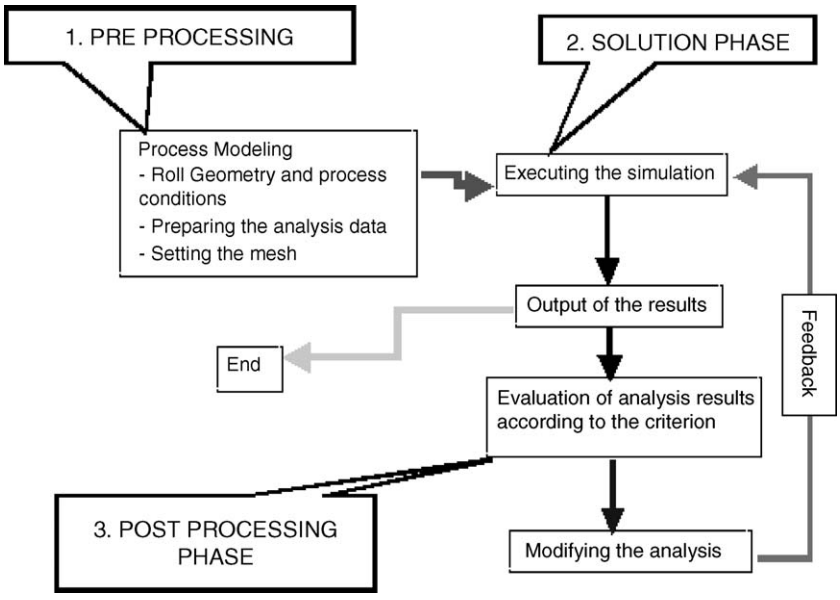

Fig. 4. SHAPE-RF algorithm.

Table 1
Entry and exit conditions

	Φ	H	K	p
Entry	a	H_0	$(R/h_f)e^{\mu H_0}$	$Y'_f(h/h_0)e^{-\mu(H_0-H)}$
Exit	0	0	R/h_f	$Y'_f(h/h_f)e^{\mu H}$

where H is given by:

$$H = 2\sqrt{\frac{R}{h}\tan^{-1}}\left(\phi\sqrt{\frac{R}{h}}\right) \tag{11}$$

The principal stresses (p) at entry and exit conditions are given in Table 1.

2. FE simulation software for roll forming

SHAPE-RF, the finite element simulation software for roll-forming process [4], employs a three-dimensional rigid-plastic finite element method and adopts an initial guessing algorithm from the two-dimensional finite element model of the pre-estimated section to find steady state solutions, thereby reducing simulation times.

SHAPE-RF can reduce the lead-time and the cost during a product and process development by eliminating unnecessary tryouts through computer simulations which verifies product, roll and process designs, and predicts potential defects of products as shown in Fig. 4.

2.1. Pre-processing phase

To initiate a simulation, the required inputs are:

(1) number of passes;
(2) roll designs (import from a CAD database);
(3) initial section geometry (can be imported or created);
(4) roll properties (velocities, friction);
(5) pass properties (central alignment, horizontal offsets);
(6) process conditions (hot forming or cold forming);
(7) welding pass.

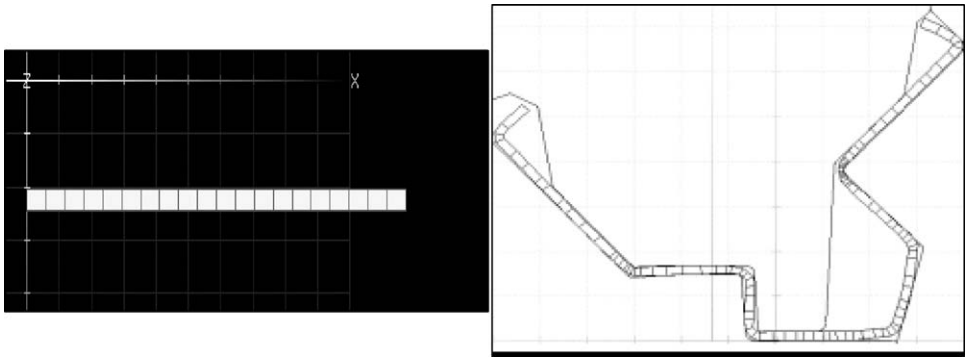

Fig. 5. Mesh for a simple and a complex section.

2.2. Solution phase

There are two most widely used solvers in finite element analysis: Skyline solver and Sparse solver. Sparse solver usually works faster than the Skyline solver.

Sparse matrices computations [5] are core to many important applications like solving partial differential equations using FDM, FEM discretisations. Sparse linear systems work by repeatedly improving an approximate solution until it is accurate enough. Sparse matrices are matrices in which most of the entries are zero. The goal of Skyline matrix software is to take maximum advantage of these zero entries to reduce storage and arithmetic manipulations.

Before solving the system an appropriate mesh must be defined. Initially simple meshes consisting of horizontal lines are sufficient as shown in Fig. 5. If the latter passes are com-

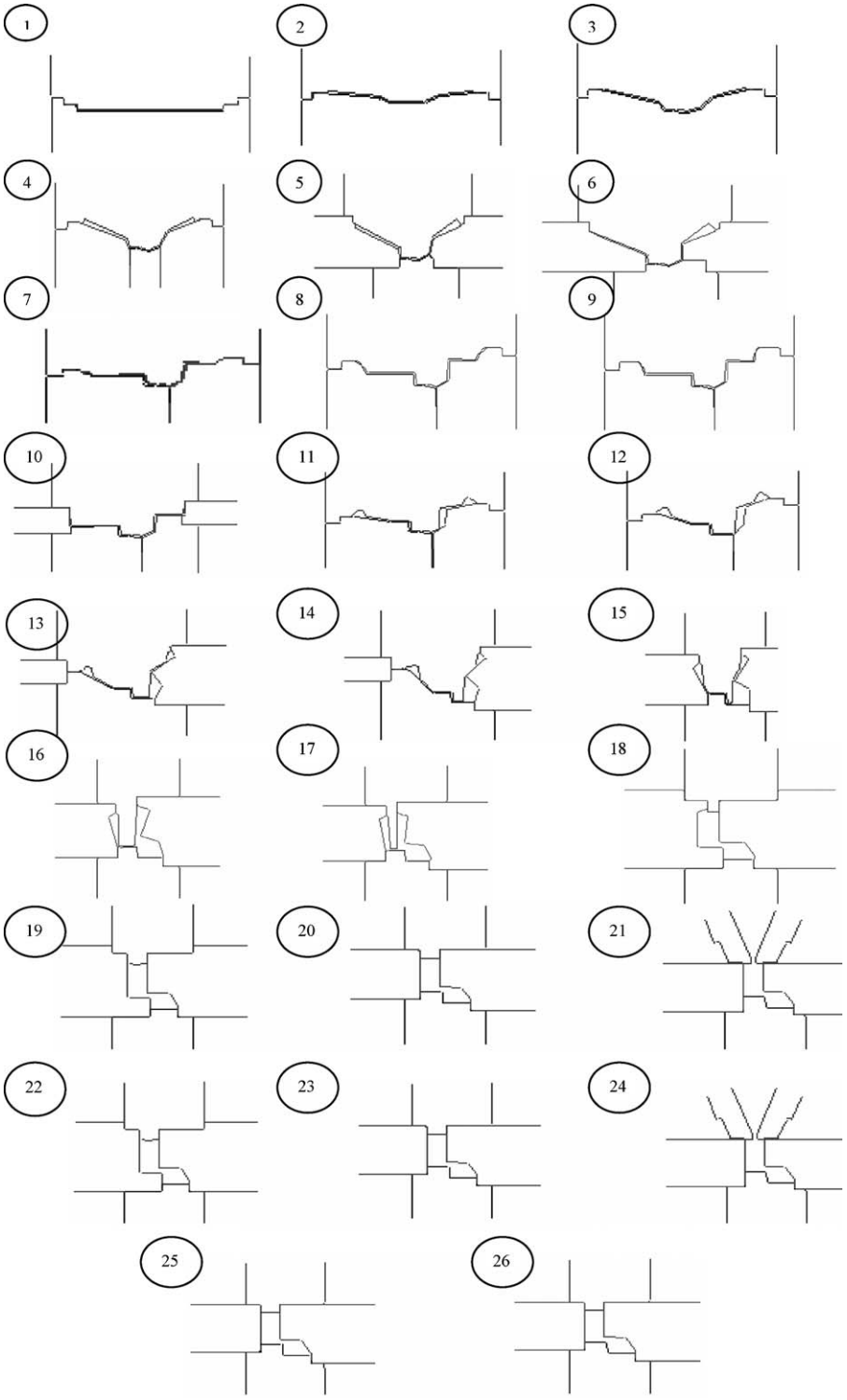

Fig. 6. Roll designs for the 26 passes.

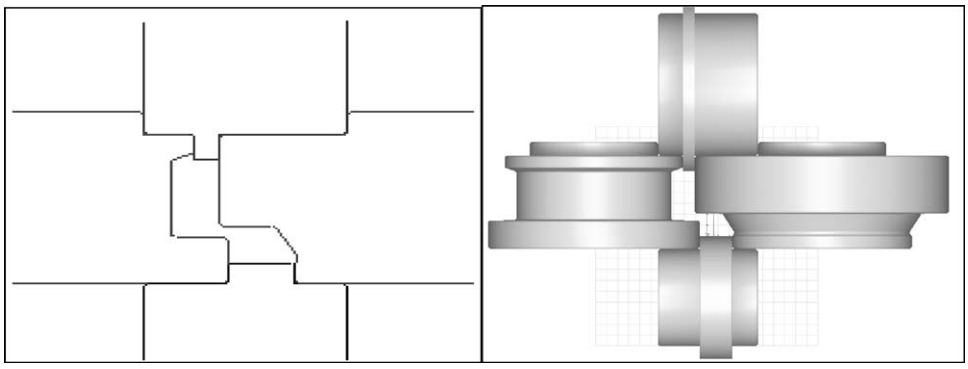

Fig. 7. Design imported into SHAPE-RF for Pass 21.

plex, the software has the provision for remeshing the section to requirements.

2.3. Post-processing phase

Post-processing phase examines the results of the analysis. Various plots can be drawn from the results to provide focus on areas of interest. Some of the results that the software can provide are:

(1) effective strain rate;
(2) strain rate;
(3) thickness;
(4) thickness stain;
(5) velocity (V_x, V_y, V_z);
(6) pressure;
(7) temperature;
(8) width strain;
(9) longitudinal strain.

3. Industrial case study

3.1. Overview

Advanced computer aided technology is required to used extensively in the development and production of cost efficient cold rolled formed sections with high standards of performance and reliability. The sections currently produced suffer from many defects due to (1) buckling, (2) spring-back, (3) piercing, and (4) 20% returned tooling.

Table 2
Bottom roll velocity profile

Pass number	Bottom pass diameter	Speed (mm/s)	Bottom revolutions/min	Bottom angular velocity (ω) (rad/s)	Bottom angular velocity (ω) (rev/s)
1	135.68	166.67	73.70	7.72	1.23
2	132.49	166.67	75.48	7.90	1.26
3	164.22	166.67	60.89	6.38	1.01
4	192.87	166.67	51.85	5.43	0.86
5	121.19	166.67	82.52	8.64	1.38
6	125.64	166.67	79.59	8.33	1.33
6A	220.00	166.67	45.45	4.76	0.76
7	125.64	166.67	79.59	8.33	1.33
8	178.49	166.67	56.03	5.87	0.93
9	193.75	166.67	51.61	5.40	0.86
10	207.34	166.67	48.23	5.05	0.80
11	209.34	166.67	47.77	5.00	0.80
12	174.77	166.67	57.22	5.99	0.95
13	196.00	166.67	51.02	5.34	0.85
14	219.78	166.67	45.50	4.76	0.76
15	190.00	166.67	52.63	5.51	0.88
16	211.02	166.67	47.39	4.96	0.79
17	141.26	166.67	70.79	7.41	1.18
18	141.26	166.67	70.79	7.41	1.18
19	141.26	166.67	70.79	7.41	1.18
20	111.76	166.67	89.48	9.37	1.49
21	111.76	166.67	89.48	9.37	1.49
22	141.26	166.67	70.79	7.41	1.18
23	141.26	166.67	70.79	7.41	1.18
24	141.26	166.67	70.79	7.41	1.18

The problem considered here consists of a 26-pass line (24 roll forming passes, 1 welding pass and 1 lifting pass). The process requires a high degree of consistency and accuracy, producing to any desired length from a wide range of materials. The RF software has been used here to model and simulate the pass line and the output compared with industrial results for a technical assessment.

3.2. Application of SHAPE-RF

SHAPE-RF is the latest development in the area of roll-forming process. It can simulate the roll-forming process quite efficiently which would not be possible for any general-purpose finite element package. A variety of sections and tubes can be simulated and the results obtained for field variables such as effective strain, strain rate, longitudinal strain, pressure, temperature, velocities, thickness and width strains, etc. It provides sufficient roll pass information for each pass including: separating force, thrust force, driving torque and coefficient of friction. Buckling analysis and spring-back analysis can also be performed effectively. Laser welding can be applied at the end of the process. Any number of passes can be created to simulate the actual process of roll forming as the rolls can be imported or created. It has good post-processing capabilities like curve plotting, flow net, and creating sliced work-piece. The simulation can be restarted from any point of time and the process parameters can be changed. Comparisons between the pre-estimated section and the actual rolled section can also be made.

3.2.1. Pre-processing

The required information for setting up the simulation include: roll designs, initial section profile and process related information.

3.2.1.1. Roll design. This is imported from a CAD package as shown in Fig. 6 for all the 26 passes. Fig. 7 elaborates this for the 21st pass in the process.

3.2.1.2. Pass properties. Once the rolls are imported they are centralized and positioned accurately. The required inputs are:

(a) horizontal distance between the rolls = 270 mm;
(b) uphill or downhill process;
(c) entry angle;
(d) welding pass number = 24th pass;

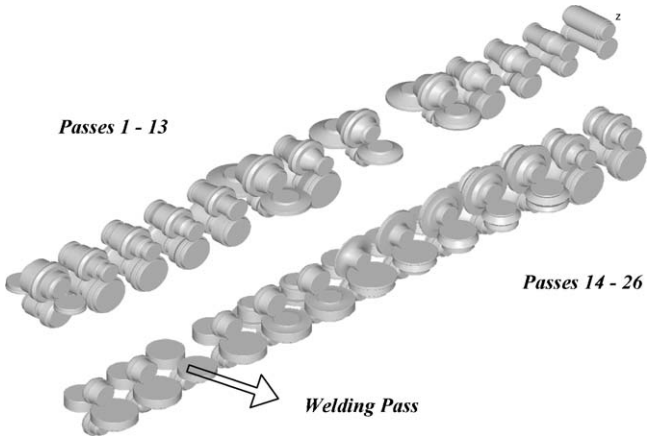

Fig. 8. Process set-up.

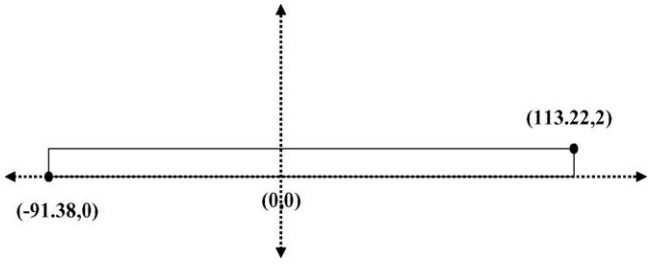

Fig. 9. Initial section geometry.

All these inputs produce a set-up as shown in Fig. 8.

3.2.1.3. Roll properties. The process environment is defined with the following key parameters:

(a) roll velocities: values are given in Tables 2 and 3;
(b) surface temperature of rolls: 300 K;
(c) cold forming process;
(d) coefficient of friction: 0.01.

3.2.1.4. Workpiece or initial section. The dimensions for the initial non-symmetric section are:

- length = 896 mm (tolerances = +4 mm, −0 mm);
- initial strip width = 204.6 mm;
- thickness of material = 2.0 mm.

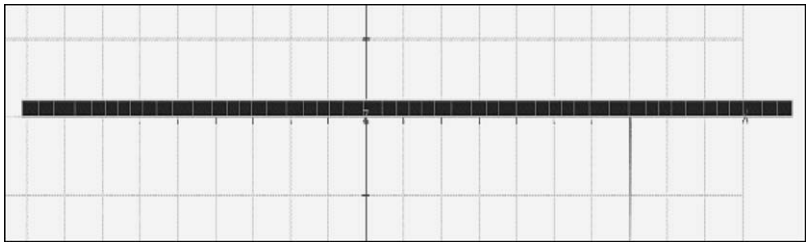

Fig. 10. Initial section profile in SHAPE-RF.

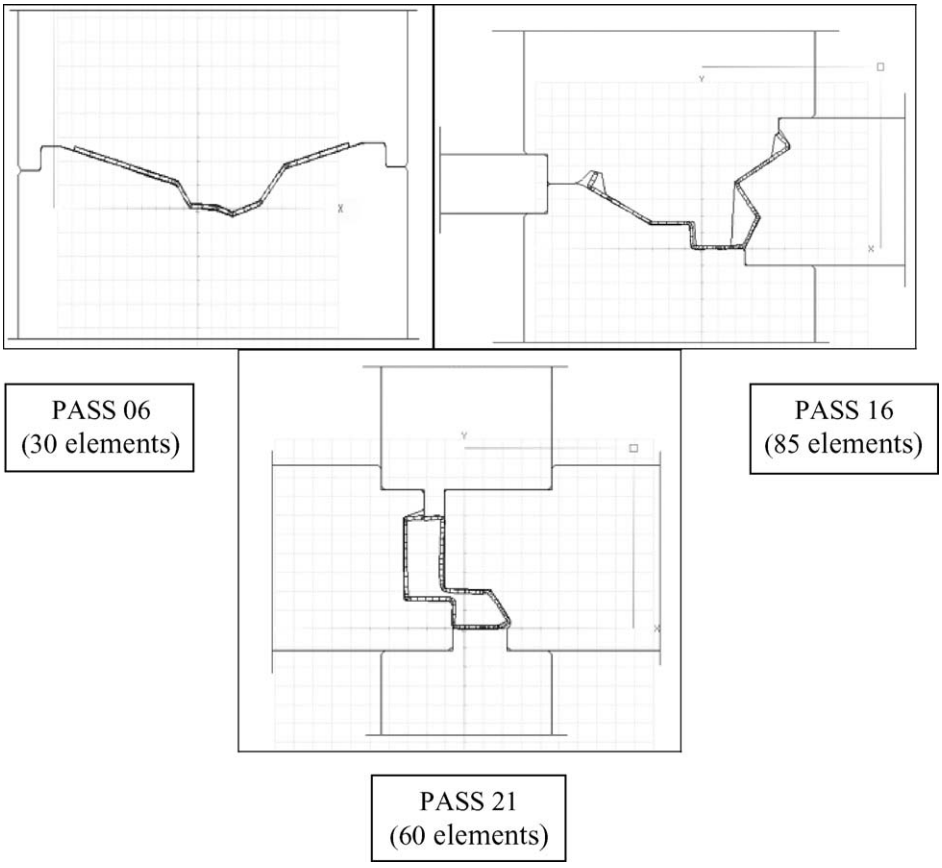

Fig. 11. Various meshing elements used in the case study.

Table 3
Top roll velocity profile

Pass number	Top pass diameter	Speed (mm/s)	Top revolutions/min	Top angular velocity (ω) (rad/s)	Top angular velocity (ω) (rev/s)
1	132.32	166.67	75.57	7.91	1.26
2	129.80	166.67	77.04	8.07	1.28
3	167.00	166.67	59.88	6.27	1.00
4	187.94	166.67	53.21	5.57	0.89
5	121.19	166.67	82.52	8.64	1.38
6	0.00	166.67	0.00	0.00	0.00
6A	193.28	166.67	51.74	5.42	0.86
7	0.00	166.67	0.00	0.00	0.00
8	171.34	166.67	58.36	6.11	0.97
9	171.34	166.67	58.36	6.11	0.97
10	184.04	166.67	54.34	5.69	0.91
11	184.04	166.67	54.34	5.69	0.91
12	0.00	166.67	0.00	0.00	0.00
13	186.54	166.67	53.61	5.61	0.89
14	192.76	166.67	51.88	5.43	0.86
15	0.00	166.67	0.00	0.00	0.00
16	0.00	166.67	0.00	0.00	0.00
17	0.00	166.67	0.00	0.00	0.00
18	0.00	166.67	0.00	0.00	0.00
19	0.00	166.67	0.00	0.00	0.00
20	0.00	166.67	0.00	0.00	0.00
21	0.00	166.67	0.00	0.00	0.00
22	0.00	166.67	0.00	0.00	0.00
23	0.00	166.67	0.00	0.00	0.00
24	0.00	166.67	0.00	0.00	0.00

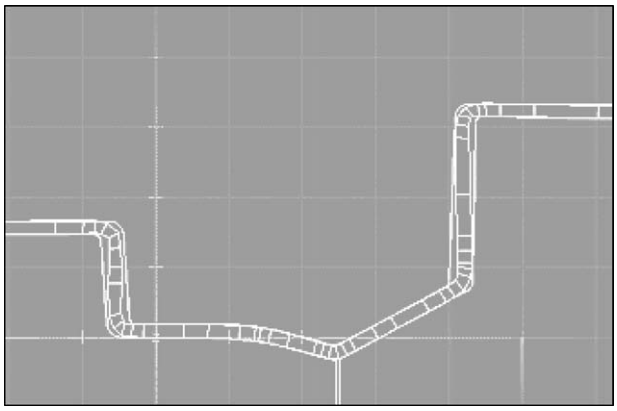

Fig. 12. Fine mesh across the bends.

The initial section is shown in Fig. 9. A mesh of 20 elements is now generated for the profile as shown in Fig. 10. This mesh can be modified to any number of elements depending on the complexity of the problem. For the current problem, passes 1–11 contain 30 elements; passes 12–20 has 85 elements and passes 20–26 are defined by 60 elements. An example for each element range is shown in Fig. 11.

It can be seen that the mesh varies at different locations in a given single pass itself, i.e. the elements are not equally spaced. This refinement around the bends is required as the passes become complex as shown in Fig. 12.

3.2.2. Solution

The next stage after setting the rolls and the process environment is to solve the system. The system under study is solved here using three different methods to find the best solution. The mathematical analysis, however, is the same for the three methods which are:

(1) Solution using a single mesh for all the passes.
(2) Solution using post-estimated section after every pass.
(3) Solution using pre-estimated sections.

3.2.2.1. Solution using a single mesh for all the passes. This method has simple solution steps, as it does not involve any remeshing or stopping of the simulation process. The single mesh that is used here for all the passes is based upon the final section to be formed. A fine mesh is concentrated on the bends of

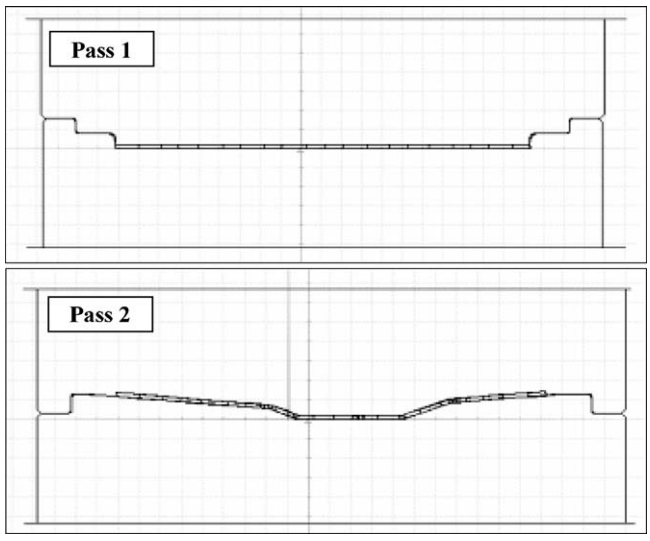

Fig. 15. Improved mesh for Pass 02 compared to Pass 01.

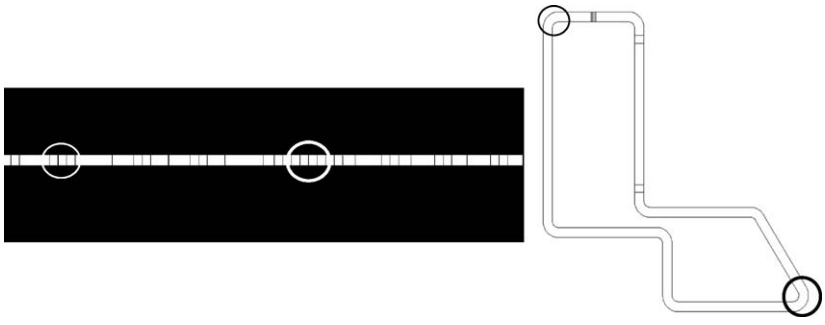

Fig. 13. Initial mesh corresponding to the final section.

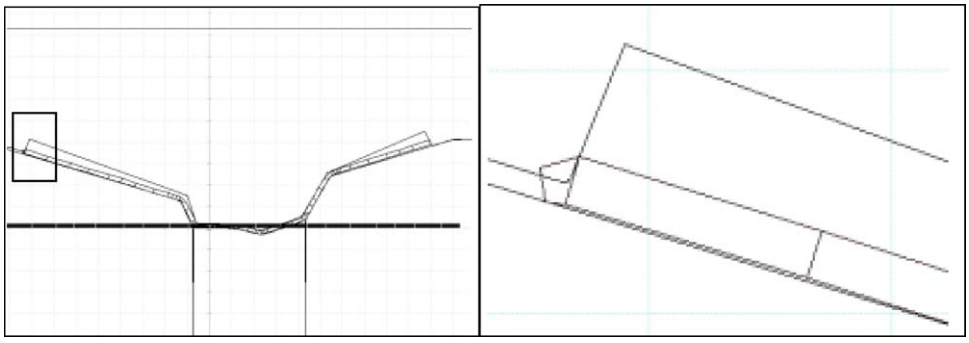

Fig. 14. Overlap occurring at Pass 04.

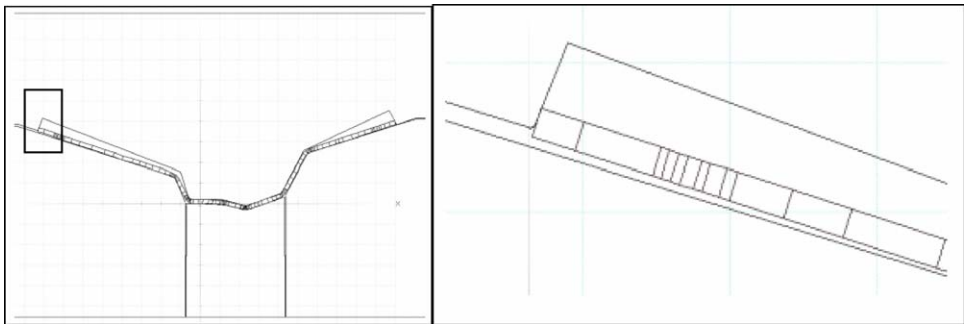

Fig. 16. No overlap occurring at Pass 04.

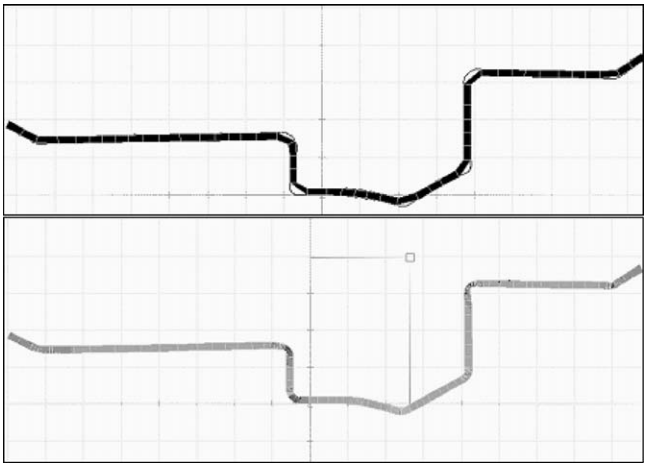

Fig. 17. Pre-estimated section and post estimated section (after solution)-Pass 10.

the final section while the straight sections were given a coarse mesh, as shown in Fig. 13.

Although this method was the easiest, the solutions achieved were not accurate and produced several overlapping (Fig. 14) and thinning instances.

3.2.2.2. Solution using post-estimated section after every pass. The second solution run involved the post-estimated section of each pass. After setting a mesh for an individual pass and running it, the process was improved by setting a new mesh corresponding to the new pass. This involved extensive remeshing after every pass (Fig. 15). Although the procedure was exhausting the results obtained were accurate and produced no instances of overlapping as shown in Fig. 16. However, the running and solution time was very high (38 h).

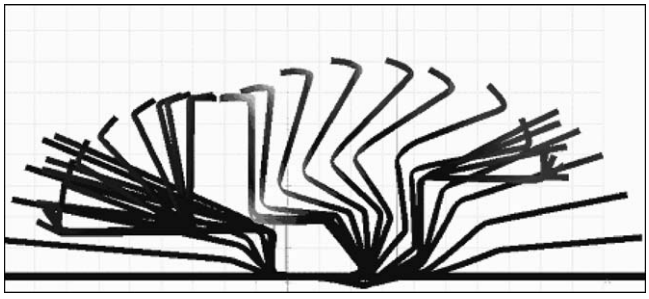

Fig. 18. Flower pattern (Pass 1–Pass 26 sections).

3.2.2.3. Solving using pre-estimated sections. Another solution procedure involved the utilisation of pre-estimated sections. Pre-estimated sections are the ideal sections to be formed after every pass. These sections are independent of the process conditions and are solely dependent on the user design. These were imported into the process along with the roll dies. For the solution an initial guess is taken from the pre-estimated section and based on it the system is solved, as shown in Fig. 17. This reduced the required mesh and the results produced (Figs. 18, 20, 21) were very close to the ideal sections. The solution time was also considerably reduced (Fig. 19).

3.2.3. Post-processing

The two field variables examined for this case study are: strain rate and thickness.

3.2.3.1. Effective strain rate. It can be seen in Fig. 22 that the strain rate reached a maximum value of 2.39 at the edge due to the thinning produced during the roll forming. This is because the section is raised at large angles in subsequent passes. It can be seen from Fig. 23 that the section is formed from Pass 16 to

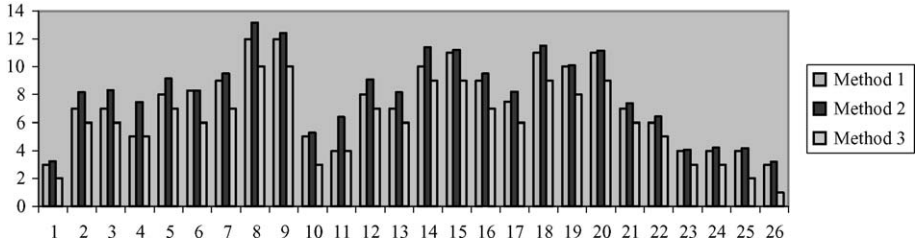

Fig. 19. Variation of solution times/pass for the three methods.

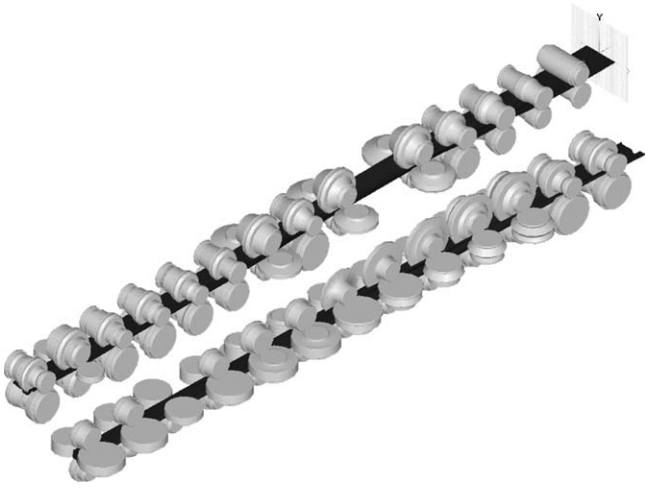

Fig. 20. Set-up with the material flowing through the dies.

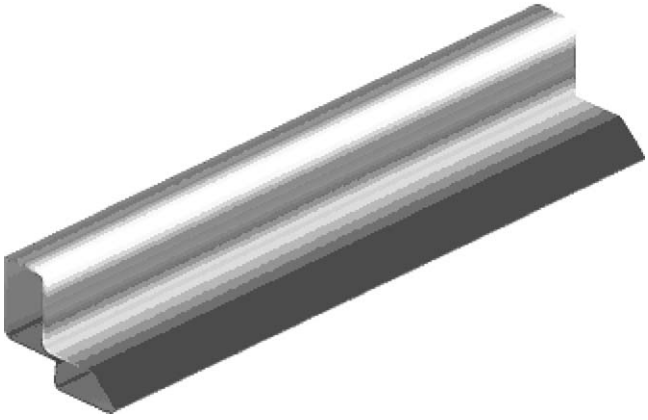

Fig. 21. Final section of the RF product.

Pass 19 at large steps, thus causing a thinning of the material at that edge. This strain is undesirable because the material fails due to piercing at this edge. This is also found to occur in the actual industrial roll process.

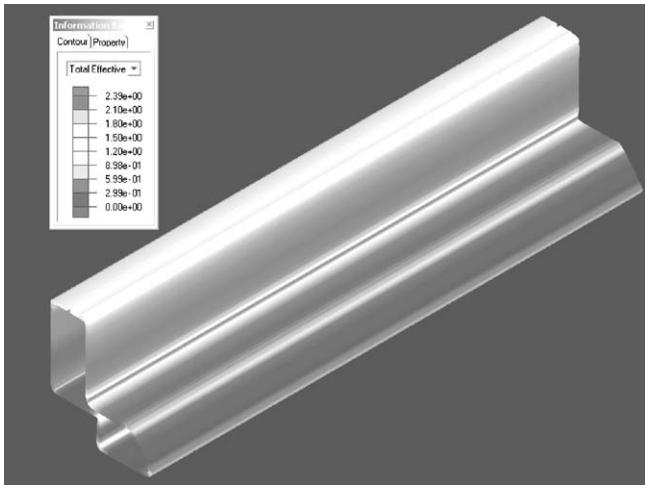

Fig. 22. Effective strain rate on the final section.

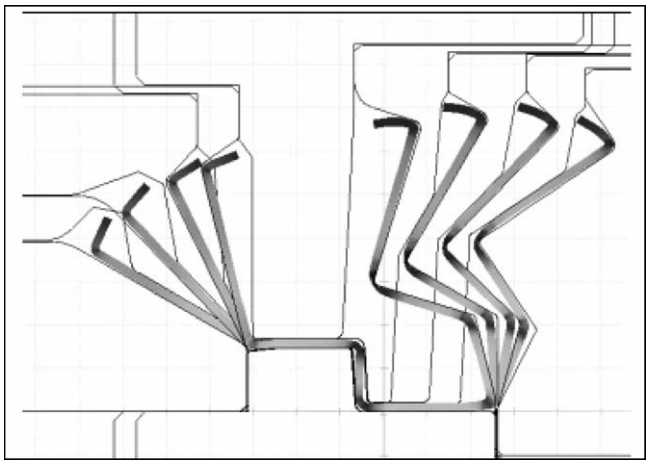

Fig. 23. Raising the material from Pass 16 to Pass 19.

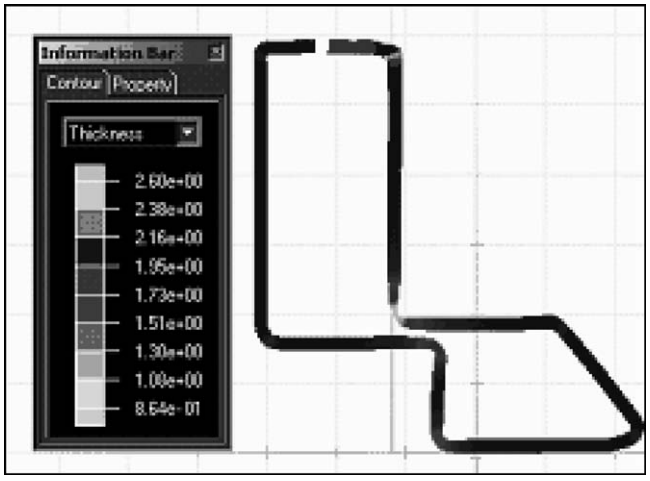

Fig. 24. Thickness variation in the final section.

3.2.3.2. Thickness. The requirement for the final section is to have a uniform thickness of 2.0 mm. However, the thickness obtained from the solution here varies across the section. The major variation is at the edge corresponding to the maximum strain rate. A thickness value of 1.00 is obtained in this region.

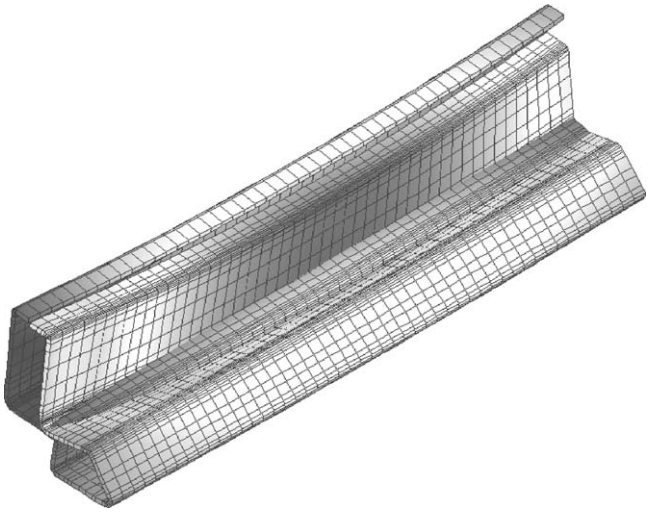

Fig. 25. Buckling analysis.

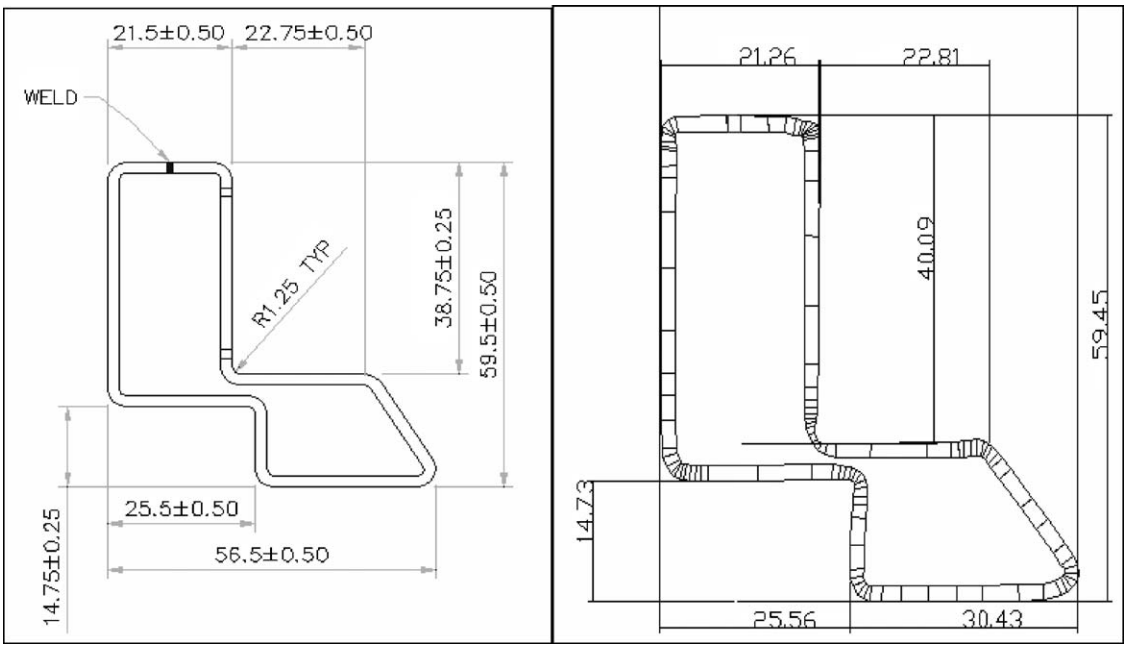

Fig. 26. Dimensional comparison between the ideal and the simulated sections.

The other regions of the section maintained a thickness within 1.90–2.10 range as shown in Fig. 24.

3.2.4. Benchmark

One of the main difficulties in the machine shop with this section arises during the piercing process. This is due to the tearing of the material in regions of high strain. The ability of the software to provide a buckling analysis is also helpful to understand where the material is weak and expected to tear. This analysis shows that the region highlighted in Fig. 25 is most likely to fail. This is due to the high strains at the edge. This explanation is validated by the evidence from the shop floor trials where the section tears during the piercing process across that section.

The final section produced is within the dimensional tolerances of the required section. On the shop floor the workpiece was identical to the simulated model, except for small variations in the dimensional values. This comparison is made in Fig. 26.

SHAPE-RF clearly identified the defects of the industrial process with its efficiency established by the benchmark. The simulation times were many times better compared to MARC software, the comparison is given in Table 4.

Table 4
Comparison between MARC and SHAPE-RF

	MARC 7.0	SHAPE-RF
Pre-processing time	2–3 days	1–2 h
Calculation time	8 h	1/2–1 h
Cost	1	0.2
Analysis range	Ordinary structure analysis	Only use the roll form process
Assumptions for analysis	Ignores friction, ignores roll rotating effect, pulling work-piece, non-steady state	With friction, without rotating effect, steady state condition

4. Conclusions

Advantages of SHAPE-RF [4] can be summarised as follows:

- SHAPE-RF gives information about the roll forces and moments for each pass as well as buckling and spring-back analysis.
- Rolls can be imported or created manually. Any number of passes can be created to simulate the actual process of roll forming.
- After the welding conditions, thick section conditions can be applied.
- Heat transfer condition can also be applied.
- The simulation can be re-started from any step and allows changing the process parameters. This helps to change the roll geometries at any step to check the improvement in the process.
- It has good post-processor capability like curve plotting, flow net, sliced work-piece, etc.

There are some areas where the software can be improved:

- The simulation time is a bit longer.
- Rolls are considered rigid.
- Information about the stresses in the rolls and formed roll are not available.
- The material database is small.
- The wear of the roll cannot be determined.
- Pierced sections cannot be analysed.

References

[1] P.Eng. Dako Kolev, Roll Forming General Overview, Kolev Industries, UK, 2001.
[2] B.F. Kuvin, Roll forming tooling—from design to production, tooling technology, Metal Forming (2002) 54–58.
[3] M. Sheikh. Roll forming analysis, Lecture Notes–Computer Aided Modelling of Materials in Manufacture, UMIST, 2004.
[4] http://www.shape.co.kr (12.07.2004).
[5] http://www.inf.ethz.ch/personal/chinella/education/parnum/files/slides/7.pdf (15.07.2004).